



Supplement of

Multi-Machine Learning Ensemble Regionalization of Hydrological Parameters for Enhancing Flood Prediction in Ungauged Mountainous Catchments

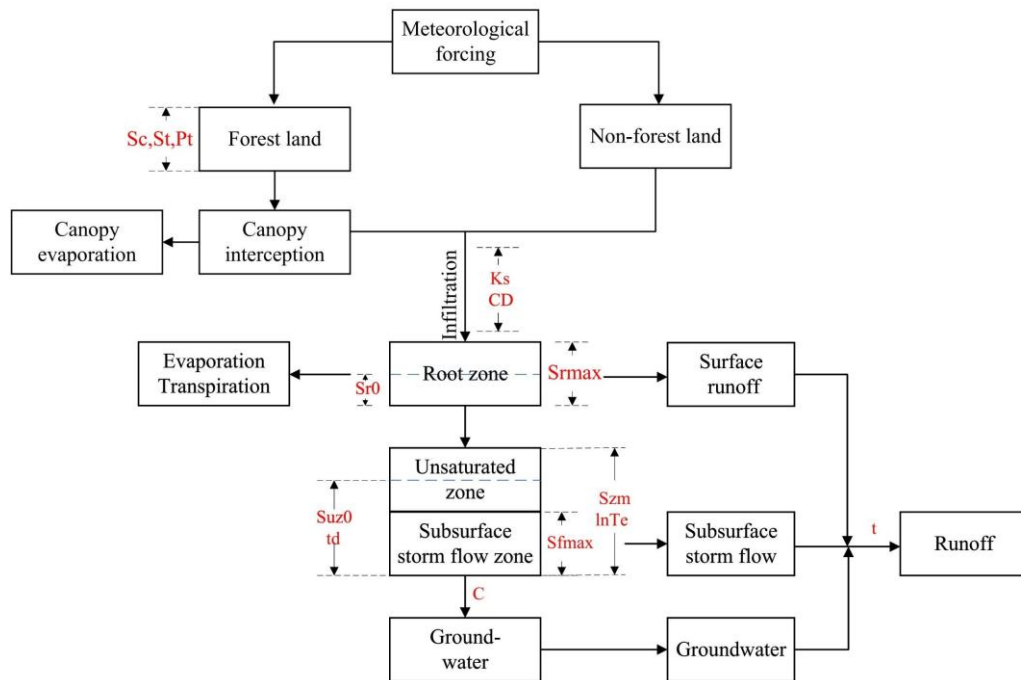
Kai Li et al.

Correspondence to: Genxu Wang (wanggx@scu.edu.cn) and Jihui Gao (jgao@scu.edu.cn)

The copyright of individual parts of the supplement might differ from the article licence.

1 **S1. The Topography-based Subsurface Storm Flow Hydrological
2 Model (Top-SSF model)**

3 The Topography-based Subsurface Storm Flow Hydrological Model (Top-SSF
4 model) is a process-based model developed to simulate the hydrological response of
5 mountainous catchments, with a particular emphasis on flash flood. The model structure
6 (Fig. S1) and its key components are detailed in the subsequent sections.



8 **Fig S1.** Schematic diagram of the Top-SSF model structure

9 **S1.1 Canopy Interception**

10 Canopy interception is calculated based on measured rainfall data and forest cover
11 characteristics. The process is divided into three distinct phases: canopy wetting,
12 canopy saturation, and canopy drying. In the Top-SSF model, the 1995 Gash model
13 (Gash et al., 1995) was modified and used as the canopy interception module. The
14 improved parts are as follows.

15 During the canopy humidification period, (1) the total interception equation for
16 calculating the rainfall events was converted to the hourly canopy interception equation
17 (Eq. 3), and (2) the total trunk runoff equation for calculating rainfall events was
18 converted to the hourly trunk runoff equation (Eq. 4).

19 $P'_g = -(\bar{R}/\bar{E})S_c \ln(1 - \bar{R}/\bar{E})$ (S1)

20 $P''_g = \bar{R}/(\bar{R} - \bar{E})(S_t/P_t) + P'_g$ (S2)

21 $I(t) = \begin{cases} cP_g(t) & (P_g(t) < P'_g) \\ cP'_g + c\bar{E}(P_g(t) - P'_g)/\bar{R} + S_t & (P_g(t) \geq P''_g) \\ cP'_g + cP_t(1 - \bar{E}/\bar{R})(P_g(t) - P'_g) + c\bar{E}(P_g(t) - P'_g)/\bar{R} & (P_g(t) > P'_g, P_g(t) < P''_g) \end{cases}$ (S3)

22 $SF(t) = \begin{cases} 0 & (P_g(t) < P'_g) \\ cP_t(1 - \bar{E}/\bar{R})(P_g(t) - P'_g) - cS_t & (P_g(t) \geq P''_g) \\ 0 & (P_g(t) > P'_g, P_g(t) < P''_g) \end{cases}$ (S4)

24 where: P'_g is the minimum rainfall required for the canopy to reach saturation (mm); \bar{R}
 25 is the average rainfall intensity (mm/h); \bar{E} is the average potential evaporation rate of
 26 the canopy (mm/h); S_c is the canopy storage capacity (mm); P''_g is the minimum
 27 rainfall needed in the trunk to reach saturation (mm); S_t is the trunk storage capacity
 28 (mm); P_t is the trunk runoff coefficient (%); $I(t)$ is the canopy interception
 29 (mm); $P_g(t)$ is the rainfall (mm); $SF(t)$ is the trunk runoff (mm); and c is the forest
 30 canopy closure (%), which is equal to the forest cover.

31 During the canopy saturation period, canopy interception and trunk interception
 32 are equal to zero, and canopy evaporation can be estimated as potential
 33 evapotranspiration using the Penman–Monteith equation (Rutter et al., 1971).

34 During the canopy dry period, the original Gash model assumes that when the
 35 canopy is completely dry, the drying time exceeds 8 hours. In the Top-SSF model, Eq.
 36 S5 was used to calculate the hourly canopy evaporation:

37 $E(t) = E_p(t)(\frac{C_h(t)}{S_c})$ (S5)

38 where $E(t)$ for actual canopy evaporation (mm); $C_h(t)$ is the depth of water held on
 39 canopy at time t (mm).

40 **S1.2 Soil Infiltration**

41 In this study, infiltration is simulated using the Green-Ampt model. When surface
 42 ponding occurs, the infiltration rate is determined by solving the Green-Ampt equation
 43 iteratively, for which the Newton-Raphson method is employed. The infiltration rate

44 (f_{in}) is given by:

45
$$f_{in} = -\frac{Ks(CD+F_{satrt})}{Szm(1-\exp(F_{satrt}/Szm))} \quad (S6)$$

46 where, f_{in} is the infiltration rate (m/h); Ks is surface hydraulic conductivity (m/h);
47 CD is capillary drive (m); F_{satrt} is the initial cumulative infiltration (m); Szm is the
48 maximum water storage capacity in the unsaturated zone (m).

49 **S1.3 Runoff Generation and Storage Dynamics**

50 **S1.3.1 Soil Evaporation**

51
$$E_a = E_{pt}(1 - \frac{Sr_z}{Sr_{max}}) \quad (S7)$$

52 where, E_a is the Actual soil evapotranspiration (m); E_{pt} is the potential
53 evapotranspiration (m); Sr_z is the root zone water deficit (m); Sr_{max} is the maximum
54 water storage capacity of the root zone (m).

55 **S1.3.2 Overland Flow**

56 Overland flow in the Top-SSF model consists of saturation-excess and infiltration-
57 excess components.

58 Saturation-excess flow: Occurs when groundwater table depth $S_i \geq 0$ at
59 computational cell i :

60
$$r_{s,i} = \max\{Suz_i - \max(S_i, 0), 0\} \quad (S8)$$

61 where $r_{s,i}$ is the depth of saturation excess overland flow generated at cell i (m);
62 Suz_i is the soil water storage in the unsaturated zone, at cell i (m); S_i is the
63 groundwater table depth at cell i (m).

64 Infiltration-excess flow: Activated when rainfall intensity exceeds soil infiltration
65 capacity.

66 **S1.3.3 Subsurface storm flow**

67 Water deficit in subsurface storm flow zone ($S_{sf,i}$) is determined by topographic
68 controls:

69
$$S_{sf,i} = S_{fmax} - \frac{\left(\frac{a}{\tan \beta}\right)A_i}{\int_A \left(\frac{a}{\tan \beta}\right) dA_i} (S_{fmax} - \bar{S}_{sf}) \quad (S9)$$

70 where, $S_{sf,i}$ is the water deficit in the subsurface storm flow zone at cell i (m); S_{fmax}

71 is the maximum subsurface storm flow zone deficit (m); $\frac{a}{\tan \beta}$ is the subsurface
 72 topographic index (-); \bar{S}_{sf} is the average water deficit in the subsurface storm flow
 73 zone (m); A_i is the percentage of the catchment area occupied by cell i (%).

74 The unsaturated zone recharges the subsurface storm flow zone:

$$75 \quad r_{v,i} = \frac{S_{uzi}}{S_t t_d} \quad (\text{S10})$$

76 where, $r_{v,i}$ is the depth of unsaturated zone recharges the subsurface storm flow zone
 77 at cell i (m); t_d is the unsaturated zone time delay per unit storage deficit (h/m).

78 The depth of storm subsurface flow generated at computational cell i , $r_{sf,i}$ is
 79 given by:

$$80 \quad r_{sf,i} = q_{sf0} (1 - S_{sf,i}/S_{fmax}) \quad (\text{S11})$$

81 where, $r_{sf,i}$ is the depth of subsurface storm flow at cell i (m); q_{sf0} is initial
 82 subsurface storm flow (m); $S_{sf,i}$ is the water storage deficit in the subsurface storm
 83 flow zone at cell i (m).

84 The subsurface storm flow recharges the groundwater:

$$85 \quad r_{g,i} = \min (C(S_{famx} - S_{sf,i}), S_i) \quad (\text{S12})$$

86 where, $r_{g,i}$ is the subsurface storm flow recharge groundwater at i (m); C is the
 87 transfer coefficient (m^2/h).

88 The average water deficit of subsurface storm flow zone (\bar{S}_{sf}) and the average
 89 depth of groundwater (\bar{S}_g) in the catchment are updated as follows:

$$90 \quad \Delta \bar{S}_{sf}/\Delta t = - \sum_{i=1}^M r_{v,i} A_i + \sum_{i=1}^M r_{sf,i} A_i + \sum_{i=1}^M r_{g,i} A_i \quad (\text{S13})$$

$$91 \quad \Delta \bar{S}_g/\Delta t = - \sum_{i=1}^M r_{g,i} A_i + r_b \quad (\text{S14})$$

92 where, $\Delta \bar{S}_{sf}$ is the change in the average subsurface storm flow zone (m); M is the
 93 total number of computational cells; $\Delta \bar{S}_g$ is the change in the average groundwater
 94 level (m); Δt is the time step (h);

95 **S1.3.4 Groundwater Flow**

96 The depth of groundwater discharge is calculate as;

97
$$r_b = e^{\ln Te - \lambda - \bar{S}_g / Szm} \quad (S15)$$

98 where, r_b is depth of groundwater discharge (m); $\ln Te$ is the log of the areal average
99 of $T0$ (m^2/h); λ is the catchment average topographic index; \bar{S}_g is the catchment
100 average groundwater table depth (m).

101 **S1.4 Flow Routing**

102 Catchment response time calculation:

103
$$T_{c,j} = t \sum_{k=1}^j \left(\frac{0.87 L_{ch,n}}{1000 S_{ch,n}} \right)^{0.385} \quad (S16)$$

104 where N is the number of river subsections within the catchment; $L_{ch,n}$ is the length
105 of the river channel (km); $S_{ch,n}$ is the slope of the river segment ($m \cdot m^{-1}$); and t is the
106 time-correction coefficient (-).

107 For any simulation time step t , the proportion of the catchment area contributing
108 to the flow at the outlet is determined. If the simulation time t is greater than or equal
109 to the time of concentration for the catchment, $T_{c,N}$ (i.e., the time of concentration
110 from the most hydrologically distant point), then the entire catchment area is assumed
111 to be contributing. Otherwise, if the simulation time t is less than $T_{c,N}$, the catchment
112 is partially contributing. The proportion of the catchment area, contributing to the outlet
113 flow at time t is calculated by linear interpolation between isochrones:

114
$$AR_t = ACH_{j-1} + \frac{t - T_{c,j-1}}{T_{c,j} - T_{c,j-1}} (ACH_j - ACH_{j-1}) \quad (S17)$$

115 where, AR_t is the proportion of the catchment area contributing to outlet flow at time t
116 (%) ; $T_{c,j}$ and $T_{c,j-1}$ are the travel times defining the boundaries of the j -th and $(j - 1)$ -th
117 isochrones, respectively (h); ACH_j and ACH_{j-1} are the cumulative proportions of
118 the total catchment area enclosed by the j -th and $(j - 1)$ -th isochrones, respectively
119 (%).

121 **S2. Hyperparameter configurations**

122 **Table S1.** DT Hyperparameter configurations

	max_depth	min_samples_split	min_samples_leaf
<i>lnTe</i>	15	9	3
<i>Szm</i>	6	4	2
<i>td</i>	18	4	2
<i>Sfmax</i>	8	6	2
<i>C</i>	18	2	1
<i>qsf0</i>	14	2	1
<i>t</i>	18	6	2

123 **Table S2.** ERT Hyperparameter configurations

	n_estimators	min_samples_split	min_samples_leaf	max_features	max_depth
<i>lnTe</i>	500	2	1	0.9	15
<i>Szm</i>	200	5	1	0.5	10
<i>td</i>	500	2	1	0.9	15
<i>Sfmax</i>	500	2	1	0.1	15
<i>C</i>	500	2	1	0.9	15
<i>qsf0</i>	400	2	1	0.1	15
<i>t</i>	500	2	1	0.9	25

124 **Table S3.** GBM Hyperparameter configurations

	subsample	n_estimators	min_samples_split	min_samples_leaf	max_depth	learning_rate
<i>lnTe</i>	1.0	800	2	1	9	0.1
<i>Szm</i>	1.0	200	2	1	3	0.1
<i>td</i>	1.0	200	2	1	4	0.1
<i>Sfmax</i>	0.8	800	2	1	9	0.1
<i>C</i>	0.6	300	2	1	5	0.05
<i>qsf0</i>	0.8	800	2	1	9	0.1
<i>t</i>	0.8	800	2	1	9	0.1

125

Table S4. KNN Hyperparameter configurations

	p	n_neighbors
<i>lnTe</i>	1	20
<i>Szm</i>	3	6
<i>td</i>	1.0	4
<i>Sfmax</i>	1	7
<i>C</i>	1	4
<i>qsf0</i>	1	30
<i>t</i>	1	5

126

Table S5. RF Hyperparameter configurations

	n_estimators	max_depth	min_samples_split	min_samples_leaf
<i>lnTe</i>	1000	10	5	1
<i>Szm</i>	100	30	4	2
<i>td</i>	100	30	5	2
<i>Sfmax</i>	200	80	2	1
<i>C</i>	1000	90	10	2
<i>qsf0</i>	700	10	2	1
<i>t</i>	500	60	2	1

127

128

Table S6. SVM Hyperparameter configurations

	tol	shrinking	kernel	gamma	C
<i>lnTe</i>	0.0001	True	rbf	10	50
<i>Szm</i>	0.0001	True	rbf	scale	0.1
<i>td</i>	0.0001	True	linear	10	1
<i>Sfmax</i>	0.0001	True	rbf	scale	0.1
<i>C</i>	0.001	True	poly	0.1	10
<i>qsf0</i>	0.0001	True	rbf	scale	0.1
<i>t</i>	0.0001	True	rbf	scale	0.1

129 **References**

130 Gash, J. H. C., Lloyd, C. R., and Lachaud, G.: Estimating sparse forest rainfall
131 interception with an analytical model, *J. Hydrol.*, 170, 79–86,
132 [https://doi.org/10.1016/0022-1694\(95\)02697-N](https://doi.org/10.1016/0022-1694(95)02697-N), 1995.

133 Rutter, A. J., Kershaw, K. A., Robins, P. C., and Morton, A. J.: A predictive model of
134 rainfall interception in forests, 1. Derivation of the model from observations in
135 a plantation of Corsican pine, *Agr. Meteorol.*, 9, 367–384,
136 [https://doi.org/10.1016/0002-1571\(71\)90034-3](https://doi.org/10.1016/0002-1571(71)90034-3), 1971.

137

138